International Journal for Housing Science and Its Applications
Publish September 11, 2025. Volume 47, Issue 1 Pages 910-920

https://doi.org/10.70517/ijhsa47179

Research on user regulation and station autonomy strategy based on particle swarm optimization algorithm in low-voltage distributed photovoltaic system

Guocheng Li[1], Cong Wang[1], Zeguang Lu[1], Ze Zhang[1,*] and Xiaoran Li[1]
[1] State Grid Dezhou Power Supply Company, Dezhou, Shandong, 253000, China
Corresponding authors: (e-mail: zhangzedq0801@163.com).

Abstract Large-scale access of distributed photovoltaic (PV) systems to low-voltage (LV) distribution networks causes voltage overruns and back-feeding problems, which seriously affect the safe and stable operation of power grids. Aiming at the voltage overrun and back-feeding overload caused by the large-scale access of low-voltage distributed photovoltaic (PV) systems, this paper proposes a user regulation and station autonomy strategy based on particle swarm optimization algorithm. A mathematical model is constructed with total power loss, voltage deviation and PV consumption ratio as the optimization objectives, and the particle swarm algorithm is used to solve the optimal access location and capacity configuration of PV system. This includes the establishment of a two-stage topology model for distributed PV systems, the design of PV MPPT control and inverter double-loop control strategies, and the use of PSO algorithm for iterative optimization of decision variables. Pilot application is carried out in a village #2 station area, and the results show that: the total voltage deviation after single-point PV optimization configuration is reduced from 1.311kV to 0.0885kV, with a voltage deviation reduction of 94.36%; the total voltage deviation of multi-point configuration is further reduced to 0.0349kV, with a reduction of 98.47%. After the implementation of the autonomous control strategy, the midday peak voltage is stabilized from over 250V to below 240V, effectively suppressing the backward flow. The optimized PV rated capacity is 970kW, which maximizes the PV consumption under satisfying the voltage constraints. It is proved that the proposed method can effectively improve the voltage quality of distribution network and guarantee the safe and efficient grid connection of distributed PV.

Index Terms Distributed photovoltaic, Particle swarm optimization, Voltage control, Station autonomy, Optimal allocation, Low-voltage distribution network

I. Introduction

Distributed photovoltaic (PV) power generation, as an emerging clean energy technology, is widely used in various power systems [1], [2]. With China's energy structure adjustment and the gradual promotion of clean energy, the application of low-voltage distributed photovoltaic (PV) systems has received more and more attention [3]. Low-voltage distributed photovoltaic system refers to the use of distributed power generation technology, the installation of photovoltaic battery packs on distributed centralized access points such as building roofs, walls, or sites, and connected to the public power grid through the low-voltage grid, supplying photovoltaic power to the power-using facilities of the buildings or sites, so as to realize self-sufficiency of electric power or power generation in parallel with the public power grid [4]-[7].

In the operation of low-voltage distributed PV systems, the safety issue is crucial [8]. The system should be equipped with perfect safety protection devices, such as lightning protection, overcurrent protection, and reverse connection protection, to ensure equipment and personal safety [9]-[11]. Meanwhile, regular safety inspection and maintenance of the system, timely detection and treatment of potential safety hazards are also the key to ensure the safe operation of the system [12], [13]. As for the complexity and practicality of low-voltage distributed photovoltaic power generation systems, the systematic design and operation of the system is needed to achieve the highest power generation conversion efficiency and energy utilization benefits [14]-[16]. Layered hierarchical design is to optimize the efficiency and performance of the system by designing the main parts of the low voltage distributed PV system, such as power generation, energy storage, and transmission, layer by layer hierarchically from top to bottom [17]-[19]. In addition, in low-voltage distributed PV systems, user regulation and station autonomy strategies can achieve grid security and efficient operation through multilevel collaborative optimization [20], [21].

Photovoltaic (PV) power generation, as an important part of clean energy, plays a key role in China's energy transition and carbon neutral strategy. Distributed photovoltaic (PV) has been developing rapidly in rural areas, and a large number of them are connected to the low-voltage distribution network, but due to the intermittent, stochastic and fluctuating characteristics of PV output, it brings serious challenges to the operation of the traditional distribution network. When the PV power generation exceeds the local load demand, it will produce power reverse flow, resulting in voltage rise at the end of the distribution network, causing equipment damage and power supply interruption in serious cases. The traditional distribution network design does not fully consider the access of distributed power sources, and lacks effective voltage regulation and control means, which makes it difficult to cope with the power quality problems under the high penetration rate of PV. Existing research focuses on the optimal allocation of photovoltaic in high-voltage distribution networks, and the research on low-voltage distribution networks, especially in rural areas, is relatively weak. Low-voltage distribution networks are characterized by large line impedance, three-phase load imbalance, and weak network structure, and the voltage problem is more prominent after PV access. Therefore, the study of distributed PV optimization control methods suitable for low-voltage distribution networks is of great significance to ensure the healthy development of PV in rural areas and the safe operation of power grids. This study proposes a control strategy based on particle swarm optimization algorithm for the voltage overrun and back-feeding overload problems caused by low-voltage distributed PV systems. Firstly, a two-stage grid-connected system model containing key equipments such as PV arrays, DC/DC converters and inverters is established to analyze the functions and control requirements of each component. Secondly, a mathematical model is constructed with the optimization objectives of minimizing network loss, minimizing voltage deviation and maximizing PV consumption ratio, and the current constraints, voltage constraints and current constraints are set. Then the particle swarm algorithm is used to solve the optimization of PV access location and capacity, and global optimization is achieved through the speed and location update formula. Finally, a typical rural station area is selected for pilot application to verify the effectiveness and practicality of the proposed strategy.

II. Low-voltage distributed photovoltaic system modeling

II. A. System architecture

Distributed photovoltaic power generation system can be divided into off-grid power generation system and grid-connected power generation system, off-grid power generation system topology only power supply and load, photovoltaic DC side is only partially connected to the load, issued by the self-generated electricity for self-use. Distributed photovoltaic power generation system grid-connected can provide active reactive power support for the grid, the current distributed photovoltaic power generation system is mainly divided into two categories according to the structure of the division, respectively, for the single-stage and two-stage, and currently more than two-stage grid-connected, its topology as shown in Fig. 1, the system consists of photovoltaic arrays, DC/DC circuits, DC buses, two-stage grid-connected inverters, loads, storage, and the power grid components.

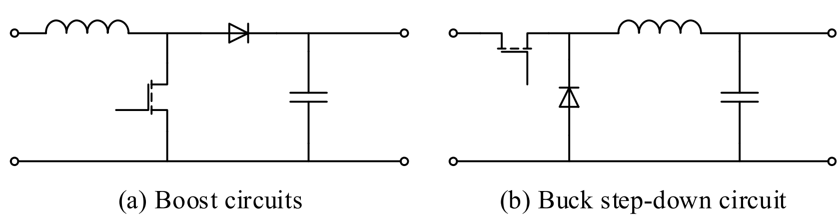

Figure 1: Topological structure

The role of the main equipment of the two-stage distributed photovoltaic power generation system is analyzed:

(1) photovoltaic array

For distributed photovoltaic power generation system power supply, the main function is to convert solar energy into electricity, the size of the current issued by the environment and the MPPT control strategy, the environmental impact, including the impact of light and temperature, light and contains a sudden change in the intensity of light and uneven light intensity, and the appropriate MPPT control strategy can ensure that the system power generation efficiency.

(2) DC/DC circuit

The MPPT control strategy mainly controls the DC/DC circuit to adjust the duty cycle by switching on and off the power electronic equipment, and the DC/DC circuit is divided into two categories: Boost boost circuit and Buck buck circuit.

1) Boost boost circuit

Distributed photovoltaic power generation system of photovoltaic arrays are often not large, the direct output voltage level is also low and unstable, Boost boost circuit can effectively enhance the voltage level, the DC/DC circuit output current ripple and the continuity inductance is small, suitable for use as an output impedance matching circuit.

2) Buck step-down circuit

In verifying the effectiveness of the MPPT method, the Buck circuit can be used, only to ensure that the battery is greater than the PV array output to avoid the complexity of the reference adjustment.

(3) Energy storage

Due to the peak power consumption and PV power generation peak is difficult to coincide, PV power generation system issued by the excess power needs to be converted to other forms of energy storage, battery as a photovoltaic power generation system storage unit, effectively reducing the direct link between the DC side and the AC side, can be unable to consume solar energy storage and release in the peak of the power consumption, power regulation to maintain the DC bus voltage, in addition to the energy storage unit can also be Bidirectional suppression of frequency, which is conducive to the stability of the power system, and if necessary, can accept the scheduling of the power grid, charging and discharging according to grid demand.

(4) Inverter and power grid

The back stage of PV power generation system consists of inverter and grid control system. Inverter as the core of PV power generation system, its control technology is also quite important, inverter through the control of IGBT on and off to make the output voltage of the positive and negative poles to change, DC power into three-phase power into the grid, can realize the tracking of the grid voltage, regulating the output power mode value and phase.

(5) DC busbar

For photovoltaic power generation system DC side output interface, can be accessed to the grid, load and energy storage, and to provide power, DC bus voltage value is also to determine the inverter on both sides of the lack of power and energy buildup of important standards, bus voltage is too high may lead to photovoltaic off-grid.

II. B.System control strategy

II. B. 1) MPPT control strategy

Swarm intelligence algorithms have both global and local search capabilities, common swarm intelligence algorithms include cuckoo algorithm, gray wolf algorithm and particle swarm algorithm [22].

Particle swarm algorithm by imitating the flight of birds global search algorithm, in the PSO algorithm, the particles have no mass and only two attributes of speed and position, the speed of the particle to determine the speed of the particle flight, and the position of the particle search direction, and its speed and position formula expression are shown in equation (1):

$$\begin{aligned} v_i(k+1) &= wv_i + c_1r_1[p_i(k) - x_i(k)] + c_2r_2[p_g(k) - x_i(k)] \\ x_i(k+1) &= x_i(k) + v_i(k+1) \end{aligned} \tag{1}$$

where w is the inertia weight,and its value is positively correlated with the global search capability. The c_1 and c_2 learning factors, c_1 is too small will make the particles prematurely fall into the local optimum. When c_2 is too small, the particles' sociality is weakened and the information sharing is low, making it difficult to find the optimal solution. r_1 and r_2 are random numbers between [0,1], P_i is the optimal position of the ith particle, and P_g is the global optimal solution.

II. B. 2) Inverter control strategy

Due to the mismatch effect of the grid voltage, the main function of the inverter is to control the inverter current for the grid-connected inverter topology, U_{dc} is the equivalent flow-controlled voltage source of the dc output voltage, and the inverter consists of six IGBT element switches, each IGBT is connected in reverse parallel with a diode; the output voltages of the inverter circuit are u_a, u_b, u_c, and the output currents are i_a, i_b, i_c. L is the AC measured filter inductor for harmonic suppression. e is the grid electric potential [23].

Taking the inverter topology as an example, let the three-phase voltage be three-phase symmetrical, the inductance L is linear and does not take into account the delay of the reaction of the power switching device, the mathematical model of the inverter in the stationary coordinates of abc can be expressed as equation (2):

$$\begin{bmatrix} u_a \\ u_b \\ u_c \end{bmatrix} = L\frac{d}{dt}\begin{bmatrix} i_a \\ i_b \\ i_c \end{bmatrix} + R\begin{bmatrix} i_a \\ i_b \\ i_c \end{bmatrix} + \begin{bmatrix} e_a \\ e_b \\ e_c \end{bmatrix} \tag{2}$$

Eq. (2) is obtained after Clark and Park transformations:

$$\begin{bmatrix} L\frac{di_d}{dt} \\ L\frac{di_q}{dt} \end{bmatrix} = \begin{bmatrix} -R & \omega L \\ -\omega L & -R \end{bmatrix}\begin{bmatrix} i_d \\ i_q \end{bmatrix} + \begin{bmatrix} 1 & 0 \\ 0 & 1 \end{bmatrix}\begin{bmatrix} u_d \\ u_q \end{bmatrix} - \begin{bmatrix} 1 & 0 \\ 0 & 1 \end{bmatrix}\begin{bmatrix} e_d \\ e_q \end{bmatrix} \tag{3}$$

The mathematical model in d and q coordinates is:

$$\begin{cases} L\frac{di_d}{dt} = -e_d + u_d - Ri_d + \omega L i_q \\ L\frac{di_q}{dt} = -e_q + u_q - Ri_q + \omega L i_d \end{cases} \tag{4}$$

From Eq. (4), it can be seen that the mathematical model of the inverter is coupled to each other in d and q coordinates, and when the current regulator is a PI controller, there is:

$$\begin{cases} u_d = -\left(K_{iP} + \frac{K_{iI}}{s}\right)(i_d^* - i_d) + \omega L i_q + e_d \\ u_q = -\left(K_{iP} + \frac{K_{iI}}{s}\right)(i_q^* - i_q) + \omega L i_d + e_q \end{cases} \tag{5}$$

where i_d^*, i_q^* are i_d, i_q current reference values, respectively. K_{iP} and K_{iI} are the current inner-loop proportional and integral gains, respectively.

In this paper, the inverter circuit control of PV inverter adopts the dual-loop control of voltage outer loop and current inner loop, the voltage outer loop sets the busbar electric reference value, stabilizes the busbar voltage near the reference value, and then carries out the static-free tracking through the PI controller, and outputs the active current reference value i_d^*; the current inner loop is used for the inverter control. The active and reactive power need to be decoupled, and the active and reactive power outputs are determined by controlling the active current reference value i_d^* and the reactive current reference value i_q^*, which is 0 under normal conditions, and the power factor of the grid-connected PV power generation system is 1.

The obtained output voltages u_d and u_q are inverted by the inverse Park transform to obtain the input voltages u_α and u_β of the input space vector pulse width modulation (SVPWM), which completes the control of the inverter. The SVPWM is divided into the sector judgment sub-module, the vector action time calculation sub-module, the vector action time selection sub-module, the switching time calculation sub-module and the PWWM sub-module. The SVPWM is divided into sector judgment sub-module, vector action time calculation sub-module, vector action time selection sub-module, switching time calculation sub-module for each sector and PWM generation sub-module.

III. PSO-based optimized control strategy for distributed PV system

III. A. Optimization model construction

Taking the total power loss, voltage deviation and PV consumption ratio of distribution network as the optimization objectives, and network current, node voltage and branch current as the constraints, the optimization model of distributed PV system is constructed.

III. A. 1) Optimization objectives

The key to the optimization model of distributed PV system is to establish the optimization model, i.e., the objective function of distributed PV optimization in the distribution system. The article establishes minimizing the total network loss, minimizing the voltage deviation and maximizing the PV consumption ratio of the distribution network as the optimization objectives [24].

Reasonable PV configuration can improve the distribution network loss, and the minimization of active loss as the optimization objective, the objective function is:

$$\min f_1 = \sum_{i=1}^{N} R_i \frac{P_i^2 + Q_i^2}{U_i^2} k_i \tag{6}$$

where, N is the total number of branch lines in the distribution network. P_i and Q_i are the active and reactive power of the i th branch line. U_i is the terminal voltage value of the i th branch line. R_i is the resistance value of the i th branch line. k_i is the switching operation of the i th branch line, with 0 representing unclosed and 1 representing closed. f_1 is the active loss.

The optimization objective of minimizing the system voltage offset is established as shown in equation (7):

$$\min f_2 = \sum_{t=1}^{k} \frac{\left(U_{ts} - U_{tN}\right)^2}{U_{tN}^2} \tag{7}$$

where, t is the node number. k is the full number of nodes. U_{ts} and U_{tN} denote the actual and rated voltage of the t th node, respectively. f_2 denotes the voltage offset.

The effective consumption E_c is used to determine the difference between the actual consumption of PV power and the system network loss:

$$E_c = \sum_{t=1}^{T} \sum_{i=1}^{H} P_{G(i,t)} - \sum_{t=1}^{T} \sum_{k=1}^{K} R_k \frac{P_{tk}^2 + Q_{tk}^2}{U_{tk}^2} \tag{8}$$

where, T refers to the number of time periods; H refers to the number of nodes connected to the power supply. $P_{G(i,t)}$ refers to the actual power consumption of node i in t time period. K is the number of closed branch lines in the system. P_{tk} , Q_{tk} and U_{tk} refer to the active power, reactive power and voltage in time period t . R_k refers to the resistance value of branch line k .

The photovoltaic equipment output P_{PV} is given in the following equation:

$$P_{PV} = \sum_{e=1}^{E} \sum_{t=1}^{T} P_{S(t,e)} h_{t\max} A_e \eta_e \tag{9}$$

In these parameters, E refers to the number of photovoltaic panels. $P_{S(t,e)}$ refers to the standardized value of the power actually injected by the e th photovoltaic panel in t time period. $h_{t\max}$ refers to the maximum light intensity at time t . A_e and η_e refer to the area of the e th photovoltaic panel and its photovoltaic conversion efficiency, respectively.

In order to reflect the relationship between the effective consumption capacity of PV power generation device and the injected power of the power generation device, and to make the optimization model more simple, the ratio of the injected power of the power generation device and the effective consumption of PV power generation device is defined as a function f_3. Then f_3 smaller and closer to 1 to prove that the better the effect of consumption, minimization of the objective function is:

$$\min f_3 = \frac{P_{PV}}{E_c} \tag{10}$$

The objective function F of the optimal scheduling model consists of a combination of 3 parts as shown in the following equation:

$$\min F = \omega_1 f_1 + \omega_2 f_2 + \omega_3 f_3 \tag{11}$$

III. A. 2) Constraints

Develop a mathematical model with current, node voltage, and branch current as constraints.

Current constraints:

$$\Delta P = P_{Gi} - V_i \sum_{j \in i} V_j \left(G_{ij} \cos\theta_{ij} + B_{ij} \sin\theta_{ij} \right) = 0 \tag{12}$$

$$\Delta Q = Q_{Gi} - V_i \sum_{j \in i} V_j \left(G_{ij} \sin \theta_{ij} - B_{ij} \cos \theta_{ij} \right) = 0 \tag{13}$$

where, P_{Gi} and Q_{Gi} represent the active and reactive power of the DG injected into the i th node; V_i refers to the maximum value of voltage at node i, and G_{ij}, B_{ij}, and θ_{ij} refer to the difference in conductance, conductivity, and phase angle of voltage between nodes i and j.

Nodal voltage constraints:

$$U_{i\min} \leq U_i \leq U_{i\max} \tag{14}$$

where, $U_{i\min}$, $U_{i\max}$ are the minimum and maximum voltage amplitudes allowed for the i th node; U_i is the value of the i th node voltage.

Branch current constraints:

$$I_l \leq I_{l\max} \tag{15}$$

where, $I_{l\max}$ is the upper limit of the branch l -carrying capacity.

The decision variables are distributed PV access location and corresponding capacity. Taking 5 access nodes and corresponding capacity as an example, the number of decision variables is 10, then its decision variable matrix VarSize is:

$$VarSize \in R^{1\times10} \tag{16}$$

In Eq. (16), VarSize is a real matrix whose columns are determined by the number of distributed PV accesses.

III. B. Design of PSO-based optimization methods

The PSO algorithm is suitable for solving problems with a continuous search space and has good convergence speed and global search capability [25]. For the optimization problem with D -dimensional search space, the initial population size is S, then the position of the first particle is $X_i\left(x_{i1}, x_{i2}, \cdots, x_{id}\right)$, and the velocity is set to $V_i\left(v_{i1}, v_{i2}, \cdots, v_{id}\right)$, the individual optimal solution of the particle in the iterative optimization process is $P_{best}\left(P_{best1}, P_{best2}, \cdots, P_{bestd}\right)$. The global optimal solution for all particles of the population is $g_{best}\left(g_{best1}, P_{best2}, \cdots, P_{bestd}\right)$, and in each iteration the particles in the population update their velocities and positions according to the following equation:

$$v_{i,d}^{k+1} = w \cdot v_{i,d}^{k} + c_1 \cdot r_1 \cdot \left(p_{best,id}^{k} - x_{i,d}^{k} \right) + c_2 \cdot r_2 \cdot \left(g_{best,d}^{k} - x_{i,d}^{k} \right) \tag{17}$$

$$x_{i,d}^{k+1} = x_{i,d}^{k} + v_{i,d}^{k+1} \tag{18}$$

where $v_{i,d}^k$ is the velocity value of the d -dimension of the i -particle in the k th iteration; $x_{i,d}^k$ is the position value of the i -particle in the d -dimension in the k th iteration; $p_{best,id}^k$ is the small optimal position obtained for the i -particle; $g_{best,id}^k$ is the global optimal position obtained in all means; w is the inertia weight; c_1 and c_2 are the acceleration coefficients; and r_1 and r_2 are the random numbers within the range of $[0,1]$.

From Eq. (17), we know that the particle velocity update includes the following three aspects:

One is $w \cdot v_{i,d}^k$, the value of this part is determined by the inertia weight w and the original velocity of the particle.

The second is $c_1 \cdot r_1 \cdot \left(p_{best,id}^k - x_{i,d}^k \right)$, which represents the particle's thinking and learning about itself.

The third part is $c_2 \cdot r_2 \cdot \left(g_{best,id}^k - x_{i,d}^k \right)$, which represents the particle's approximation of the optimal solution of the population, i.e., the social experience from the outside world, i.e., the “social part”.

When PSO is used to solve the optimization problem of distributed photovoltaic system, it is necessary to encode the particles, and each particle in the PSO algorithm can be represented by its position and speed, in the algorithm, first of all, it is necessary to encode the position of the particles appropriately, and the position of the particles represents the optimization scheme of the decision variables, i.e., the position and capacity of power supply access, and there are a total of S particles in the PSO population in the space of dimensions of d. Perform the search. The i th particle P_i is represented by its position X_i and velocity V_i. The value in X_i denotes the capacity of the distributed PV accessed in that node. The real-valued matrix of $V_i \in R^{s\times n}$ represents the magnitude of the particle's velocity, and the range of values of each element in V_i is restricted between $[v_{\min}, v_{\max}]$.

The PSO-based distributed PV system optimization process is described as follows: first, the location of distributed PV access and its capacity are initialized, and then the algorithm undergoes continuous iterative convergence until a set of solutions to the optimization problem emerges. Each solution found during the iterative process represents a feasible solution after accessing the PV, as well as a particle in the population, and the solution corresponds to a fitness value through the optimization objective function. An optimal solution found by a particle during the simulated flight of a flock of birds is called an individual optimal solution denoted by P_{best}, while the best solution searched globally by the whole population is called the global optimal solution G_{best}. Each particle in the population updates its own optimization scheme by simultaneously pursuing the individual and global optimal solutions.

IV. Typical pilot analysis of station autonomy control strategy

IV. A. Current status of the station

In this paper, a village is selected to carry out a typical pilot of autonomous autonomous strategy, a village since 2024 to carry out rural supporting grid transformation, after the transformation of the whole village average household capacity increased to 3.5kVA, line insulation rate increased to 100%, power supply reliability rate and voltage pass rate are 99.99% or more, the residents' life and agricultural production of electricity are normal, to meet the basic conditions of the pilot requirements. Since November 2023, the distributed PV load of a village #2 station ushered in explosive growth, and continued to grow after reaching the upper limit of the transformer capacity in August 2024, and now a total of 12 households are connected with PV users as shown in Fig. 2, which reached 147.63% of the rated capacity of the transformer of 200 kVA, resulting in overload of back-feeding of the station, with the maximum back-feeding load ratio of the station reaching 111.20%, which seriously affect the safe and stable operation of grid equipment, and over-voltage caused some damage to the user's electrical equipment.

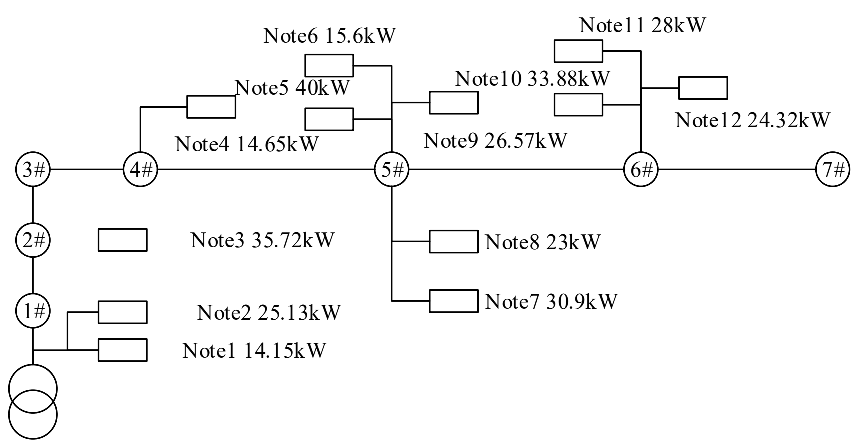

Figure 2: # 2 low voltage distributed photovoltaic access map

IV. B. Optimization of grid-connected configuration of distributed PV systems

Taking a low-voltage station area in a village low-voltage distribution network as an example, we search for the optimal access location and optimal output of the PV system to be connected to the grid, in order to achieve the purpose of improving the voltage of each node. Due to the three-phase load imbalance in this station area, trend calculation and optimal allocation of PV grid-connection must be carried out individually for each phase. In this paper, the case in subsection 4.1 is used as a study case to optimize the single-point and multi-point PV grid-connected configuration for phase A of the station area with the optimization objective of minimizing the total voltage deviation. The convergence curve of particle swarm optimization algorithm is shown in Fig. 3. There are 12 nodes and 5 branch circuits in phase A of this station, with an estimated total active load of 28.6 kW, and the voltage at node 1 is set to 0.24 kV. When the PV system is not configured, the total voltage deviation of each node of the network is 1.311 kV, and the total active loss is 6.0 kW. The single-point PV grid-connected optimization configuration, with the objective function of minimizing the total voltage deviation and the particle swarm optimization algorithm, yields the optimal position of node 12, the optimal location of the PV system connected to the network, and the optimal location of node 12. The optimal location is node 12, the optimal output is 20.474kW, the total voltage deviation is 0.0885kV, and the total active loss is 0.672kW.

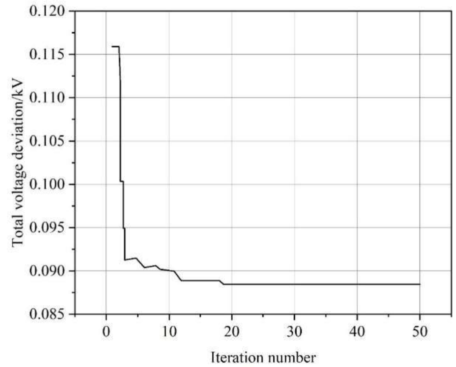

Figure 3: Particle swarm optimization algorithm convergence curve

The voltage pairs of each node using different objective functions are shown in Fig. 4.

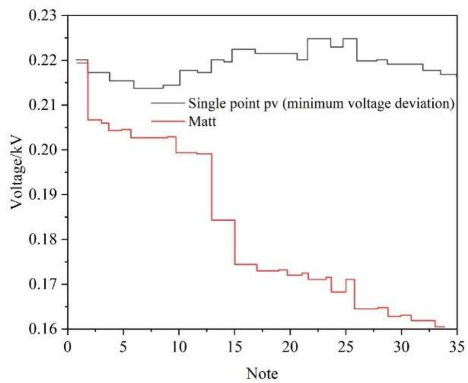

Figure 4: Each node voltage contrast of different target functions

The convergence curve of particle swarm optimization algorithm is shown in Fig. 5. The optimal configuration of multi-point PV grid-connected with minimum total voltage deviation as the objective function, using particle swarm optimization algorithm, obtains the optimal location of PV system grid-connected as node 3 and node 7, the optimal output is 10.492kW and 16.983kW, respectively, the total voltage deviation is 0.0349kV, and the total active loss is 0.422kW.

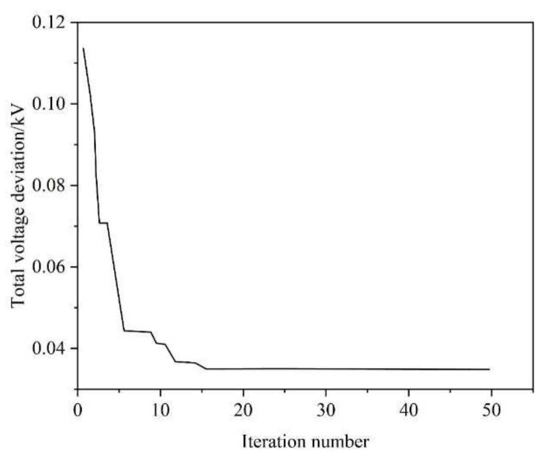

Figure 5: Particle swarm optimization algorithm convergence curve

The example of each node using different objective functions is shown in Fig. 6.

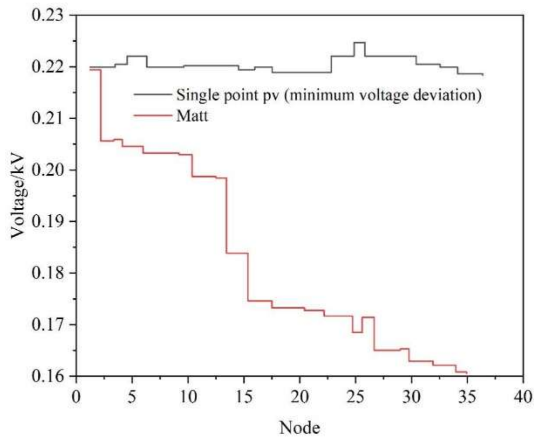

Figure 6: Each node voltage contrast of different target functions

It can be seen that the PV system grid-connected to improve the node voltage so that it basically reaches the rated voltage, reduce network losses, can be better to play a "low voltage" management effect, the results are shown in Table 1. PV grid-connected optimal configuration results for the optimal location: single-point PV node 12, multi-point PV nodes 3 and 7.

Table 1: Comparison of optimal configuration results of photovoltaic network

Target function	Matt	Single point photovoltaic	Multipoint photovoltaic
Particle swarm algorithm parameters		$c_1 = 1.5142$ $c_2 = 1.5142$ $w = 0.7324$ $MaxDT = 52$ $D = 3$ $N = 32$	$c_1 = 1.5142$ $c_2 = 1.5142$ $w = 0.7324$ $MaxDT = 52$ $D = 3$ $N = 32$
Optimal position		Node 12	Node 3 Node 7
Optimal force/kw		20.468	10.475 16.984
Net loss/kw	6.0	0.663	0.425
Total voltage deviation/kv	1.312	0.089	0.046
Voltage bias reduction rate%		94.36	98.47

IV. C. Analysis of optimization results

The optimization of distributed PV rated capacity according to the above optimization control strategy is obtained as shown in Fig. 7, where Fig. (a) indicates that ΔP is scaled down in equal steps to the rated PV rated capacity, and Fig. (b) indicates that the final iteration is 44 times, and the iteration stops when the condition of $0 < \Delta U < \Delta$, which ultimately yields the optimized rated PV capacity of 970 kW.

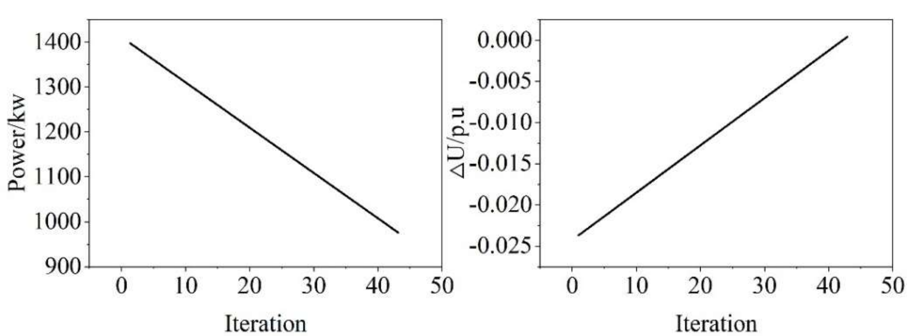

Figure 7: PV rated capacity optimization iteration and search optimization range

The voltage distribution under 24 moments of node 7 with access to distributed PV after optimization is shown in Fig. 8, and from the figure, it can be obtained that the node voltage under each moment does not exceed the constraints when the rated capacity of the accessed distributed PV is 970 kW, and from the conclusion, it can be known that when the accessed distributed PV power node does not exceed the constraints, other nodes will not exceed the constraints as well. This is the maximum rated capacity of PV that satisfies the voltage constraints.

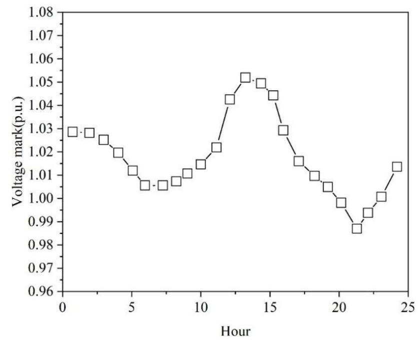

Figure 8: Optimized voltage distribution at 24 times in node 18

IV. D. Analysis of the effect of the implementation of the station autonomy strategy

In a village #2 station area to implement the previously described over the station voltage autonomy strategy, the implementation of the strategy is shown in Figure 9. Taking the end of the 6th pole and grid point as an example, the control strategy was not activated throughout the day on October 13, and the phenomenon of back-feeding occurred in the PV, resulting in a voltage peak of more than 250V at noon, which posed a hidden danger to the safety of the power supply system. Since October 14th, the autonomous control strategy has been activated, and the intelligent convergence terminal system monitors the voltage level of each node in real time and adjusts the PV output, and the curve shows that the voltage fluctuation at noon is not obvious, and the voltage level of the station area remains stable throughout the day on October 14th. When the control strategy is stopped at 14:00 on October 15, the voltage in the station area does not stabilize, and the peak voltage rises rapidly, exceeding the limit value again. From this, it can be concluded that the control strategy of autonomous autonomy has the effect of maintaining voltage stability and preventing the occurrence of tidal reversal to a certain extent.

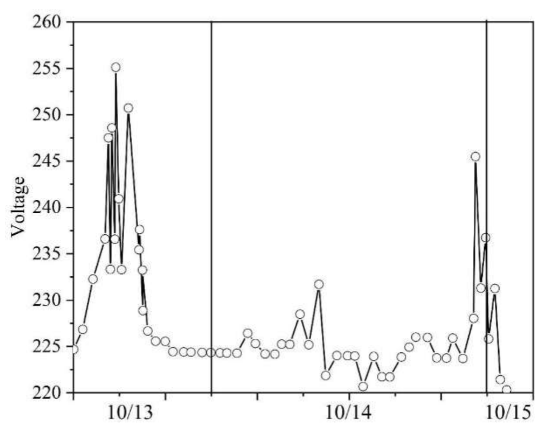

Figure 9: Implementation effect of station autonomous control strategy

V. Conclusion

The particle swarm optimization algorithm-based control strategy for low-voltage distributed PV system is applied in a village #2 station area to verify its significant effect. In terms of optimized configuration, when single-point PV is accessed at node 12 position with a capacity of 20.468kW, the total active loss of the system is reduced from 6.0kW to 0.663kW, with a loss reduction rate of 88.95%; when multi-point configuration is accessed at node 3 and node 7 with 10.475kW and 16.984kW, respectively, the network loss is further reduced to 0.425kW.Voltage quality improves significantly, and the node voltage is basically restored to the vicinity of the rated value, effectively solving the low-voltage problem. After the implementation of the station autonomy control strategy, the peak voltage at the terminal grid-connected points was controlled from over 250V to below 240V, and the voltage fluctuations throughout the day were kept within the safe range. The maximum PV access capacity of 970kW is determined through iterative optimization, which achieves the full utilization of PV resources under the system constraints. The particle swarm algorithm converges after 44 iterations, showing good optimization efficiency and stability. Practice has proved that the proposed method can not only accurately determine the optimal PV access program, but also maintain the stable operation of the power grid through real-time regulation, providing a feasible technical path for large-scale access of distributed PV in rural areas, which is of great value for the promotion of high-quality development of new energy resources in the distribution network with important engineering applications.

References

[1] Jiang, S., Wan, C., Chen, C., Cao, E., & Song, Y. (2018). Distributed photovoltaic generation in the electricity market: status, mode and strategy. CSEE Journal of Power and Energy Systems, 4(3), 263-272.

[2] Çeçen, M., Yavuz, C., Tırmıkçı, C. A., Sarıkaya, S., & Yanıkoğlu, E. (2022). Analysis and evaluation of distributed photovoltaic generation in electrical energy production and related regulations of Turkey. Clean Technologies and Environmental Policy, 1-16.

[3] Li, H., Lin, H., Tan, Q., Wu, P., Wang, C., De, G., & Huang, L. (2020). Research on the policy route of China's distributed photovoltaic power generation. Energy Reports, 6, 254-263.

[4] Koirala, A., Van Acker, T., D'hulst, R., & Van Hertem, D. (2022). Hosting capacity of photovoltaic systems in low voltage distribution systems: A benchmark of deterministic and stochastic approaches. Renewable and Sustainable Energy Reviews, 155, 111899.

[5] Vai, V., & Eng, S. (2022). Study of grid-connected PV system for a low voltage distribution system: A case study of Cambodia. Energies, 15(14), 5003.

[6] Karthikeyan, N., Pokhrel, B. R., Pillai, J. R., & Bak-Jensen, B. (2017, September). Coordinated voltage control of distributed PV inverters for voltage regulation in low voltage distribution networks. In 2017 IEEE PES innovative smart grid technologies conference Europe (ISGT-Europe) (pp. 1-6). IEEE.

[7] Gui, Y., Nainar, K., Bendtsen, J. D., Diewald, N., Iov, F., Yang, Y., ... & Stoustrup, J. (2023). Voltage support with PV inverters in low-voltage distribution networks: An overview. IEEE Journal of Emerging and Selected Topics in Power Electronics, 12(2), 1503-1522.

[8] Stringer, N., Haghdadi, N., Bruce, A., Riesz, J., & MacGill, I. (2020). Observed behavior of distributed photovoltaic systems during major voltage disturbances and implications for power system security. Applied Energy, 260, 114283.

[9] Alabri, W., & Jayaweera, D. (2021). Voltage regulation in unbalanced power distribution systems with residential PV systems. International Journal of Electrical Power & Energy Systems, 131, 107036.

[10] Bayer, B., Matschoss, P., Thomas, H., & Marian, A. (2018). The German experience with integrating photovoltaic systems into the low-voltage grids. Renewable energy, 119, 129-141.

[11] Hoang, T. T., Tran, Q. T., & Besanger, Y. (2022). An advanced protection scheme for medium-voltage distribution networks containing low-voltage microgrids with high penetration of photovoltaic systems. International Journal of Electrical Power & Energy Systems, 139, 107988.

[12] Hashemi, S., & Østergaard, J. (2017). Methods and strategies for overvoltage prevention in low voltage distribution systems with PV. IET Renewable power generation, 11(2), 205-214.

[13] Salem, W. A. A., Gabr Ibrahim, W., Abdelsadek, A. M., & Nafeh, A. A. (2022). Grid connected photovoltaic system impression on power quality of low voltage distribution system. Cogent Engineering, 9(1), 2044576.

[14] Wang, L., Yan, R., & Saha, T. K. (2019). Voltage regulation challenges with unbalanced PV integration in low voltage distribution systems and the corresponding solution. Applied Energy, 256, 113927

[15] Ciocia, A., Boicea, V. A., Chicco, G., Di Leo, P., Mazza, A., Pons, E., ... & Hadj-Said, N. (2018). Voltage control in low-voltage grids using distributed photovoltaic converters and centralized devices. IEEE Transactions on Industry Applications, 55(1), 225-237.

[16] Gao, X., Zhang, J., Sun, H., Liang, Y., Wei, L., Yan, C., & Xie, Y. (2024). A Review of Voltage Control Studies on Low Voltage Distribution Networks Containing High Penetration Distributed Photovoltaics. Energies, 17(13), 3058.

[17] Malekpour, A. R., Pahwa, A., & Natarajan, B. (2016). Hierarchical architecture for integration of rooftop PV in smart distribution systems. IEEE Transactions on Smart Grid, 9(3), 2019-2029.

[18] Li-Sheng, L., Yang, L., Hai-dong, Y., Min, H., Wen-bin, L., Shi-dong, Z., & Bin, W. (2022, September). Performance evaluation of low-voltage distributed PV systems based on multi-level analysis. In IET Conference Proceedings CP806 (Vol. 2022, No. 16, pp. 340-344). Stevenage, UK: The Institution of Engineering and Technology.

[19] Palate, B. O., Guedes, T. P., Grilo-Pavani, A., Padilha-Feltrin, A., & Melo, J. D. (2021). Aggregator units allocation in low voltage distribution networks with penetration of photovoltaic systems. International Journal of Electrical Power & Energy Systems, 130, 107003.

[20] Li, G., Wang, C., Lu, Z., Zhang, Z., Li, X., & Wang, X. (2025). A study on the integrated application of computational methods in low-voltage distributed photovoltaic user regulation and station side-end autonomy strategies. J. COMBIN. MATH. COMBIN. COMPUT, 127, 6867-6884.

[21] Li, G., Li, W., Yi, S., Liu, S., Ma, X., Liu, Z., & Pei, X. (2024, July). Research on Autonomous Control Strategy for Safe Operation of High Proportion Distributed PV Stations. In 2024 IEEE 6th International Conference on Power, Intelligent Computing and Systems (ICPICS) (pp. 788-792). IEEE.

[22] Shanshan He,Huixi Li,Yuelei Ji,Xingjian Chen,Feifei Zou & Xia Zhao. (2025). Energy-aware mobile edge device deployment in health data detection scenario: a DQN optimized firefly algorithm. Computing,107(5),115-115.

[23] Jiachuan Shi,Sining Hu,Rao Fu & Quan Zhang. (2025). Convex Optimization and PV Inverter Control Strategy-Based Research on Active Distribution Networks. Energies,18(7),1793-1793.

[24] Zhuochun Wu,Jidong Kang,Martín Mosteiro Romero,Andrea Bartolini,Tsan Sheng Ng & Bin Su. (2024). A distributionally robust optimization model for building-integrated photovoltaic system expansion planning under demand and irradiance uncertainties. Applied Energy,372,123740-123740.

[25] Hossam Eddine Glida,Chelihi Abdelghani & Sentouh Chouki. (2025). Flight tracking control of mini-drone: Flower pollination algorithm based model-free control. Proceedings of the Institution of Mechanical Engineers, Part G: Journal of Aerospace Engineering,239(6),578-592.